

## $^{228}\text{Ra}$ and $^{228}\text{Th}$ concentrations in GEOSECS Atlantic surface waters\*

YUAN-HUI LI,† HERBERT W. FEELY‡ and J. ROBERT TOGGWEILER†

(Received 15 August 1979; in revised form 26 February 1980; accepted 28 February 1980)

**Abstract**—An average  $^{228}\text{Ra}$  flux of  $0.6 \pm 0.1$  dpm  $\text{cm}^{-2}$   $\text{yr}^{-1}$  from continental shelf sediments can maintain the estimated total  $^{228}\text{Ra}$  inventory of about  $5 \times 10^{17}$  dpm in Atlantic surface waters. By fitting  $^{228}\text{Ra}$  and potential temperature data to Munk's vertical advection-diffusion model, upwelling rates of  $17 \pm 10$  m  $\text{yr}^{-1}$  and vertical eddy diffusion coefficients of  $0.4 \pm 0.2$   $\text{cm}^2$   $\text{s}^{-1}$  were obtained in the upper water column of the equatorial Atlantic. The downward fluxes of particulate  $^{228}\text{Th}$  across the 350-m water depth are about 0.01 to 0.04 dpm  $\text{cm}^{-2}$   $\text{yr}^{-1}$  in the Sargasso Sea and in the regions south of  $12^\circ\text{N}$  and about 0.06 to 0.11 dpm  $\text{cm}^{-2}$   $\text{yr}^{-1}$  in the northern temperate region (excluding the Sargasso Sea). The shorter half-removal time of  $^{228}\text{Th}$  in the equatorial ( $10^\circ\text{S}$  to  $20^\circ\text{N}$ ) and the northern region ( $35^\circ$  to  $65^\circ\text{N}$ ) are related to higher biological productivity there.

### INTRODUCTION

AS A PART of the Geochemical Ocean Sections program (GEOSECS) more than 300 large-volume water samples were collected in the Atlantic for the determination of  $^{228}\text{Ra}$  ( $t_{1/2} = 5.75$  yr) and its daughter product  $^{228}\text{Th}$  ( $t_{1/2} = 1.91$  yr). Our objectives were: (1) the measurement of  $^{228}\text{Ra}$  concentrations in profiles of near-surface and near-bottom samples to provide a basis for the estimation of rates of horizontal and vertical eddy diffusion within the surface and the bottom waters (KAUFMAN, TRIER and BROECKER, 1973), and (2) the measurement of  $^{228}\text{Th}/^{228}\text{Ra}$  ratios in profiles of near-surface water to provide a basis for estimating rates of  $^{228}\text{Th}$  removal from the surface layer by settling particles (BROECKER, KAUFMAN and TRIER, 1973).

In this paper, we present  $^{228}\text{Ra}$  and  $^{228}\text{Th}$  results from the surface layer (<350 m) of the Atlantic Ocean. The results from the bottom waters will be presented separately.

Figure 1 gives the locations of the GEOSECS Atlantic stations.

### ANALYTICAL METHODS

Unfiltered 600 to 875-l seawater samples were collected by means of a permanently mounted pump for surface samples and a submersible pump for samples to depths of 350 m. The water was placed in 900-l polyethylene tanks and acidified to pH about 4 with HCl. A solution of iron-barium carrier and  $^{230}\text{Th}$  spike (14.8 dpm) was added. Enough  $\text{NH}_4\text{OH}$  was then added to raise the pH to about 7, producing a mixed precipitate of iron hydroxide with coprecipitated thorium and barium sulfate with coprecipitated radium and

\* Lamont-Doherty Geological Observatory Contribution No. 2966.

† Lamont-Doherty Geological Observatory of Columbia University, Palisades, NY 10964, U.S.A.

‡ Department of Energy, Environmental Measurement Laboratory, 376 Hudson Street, New York, N.Y., U.S.A.

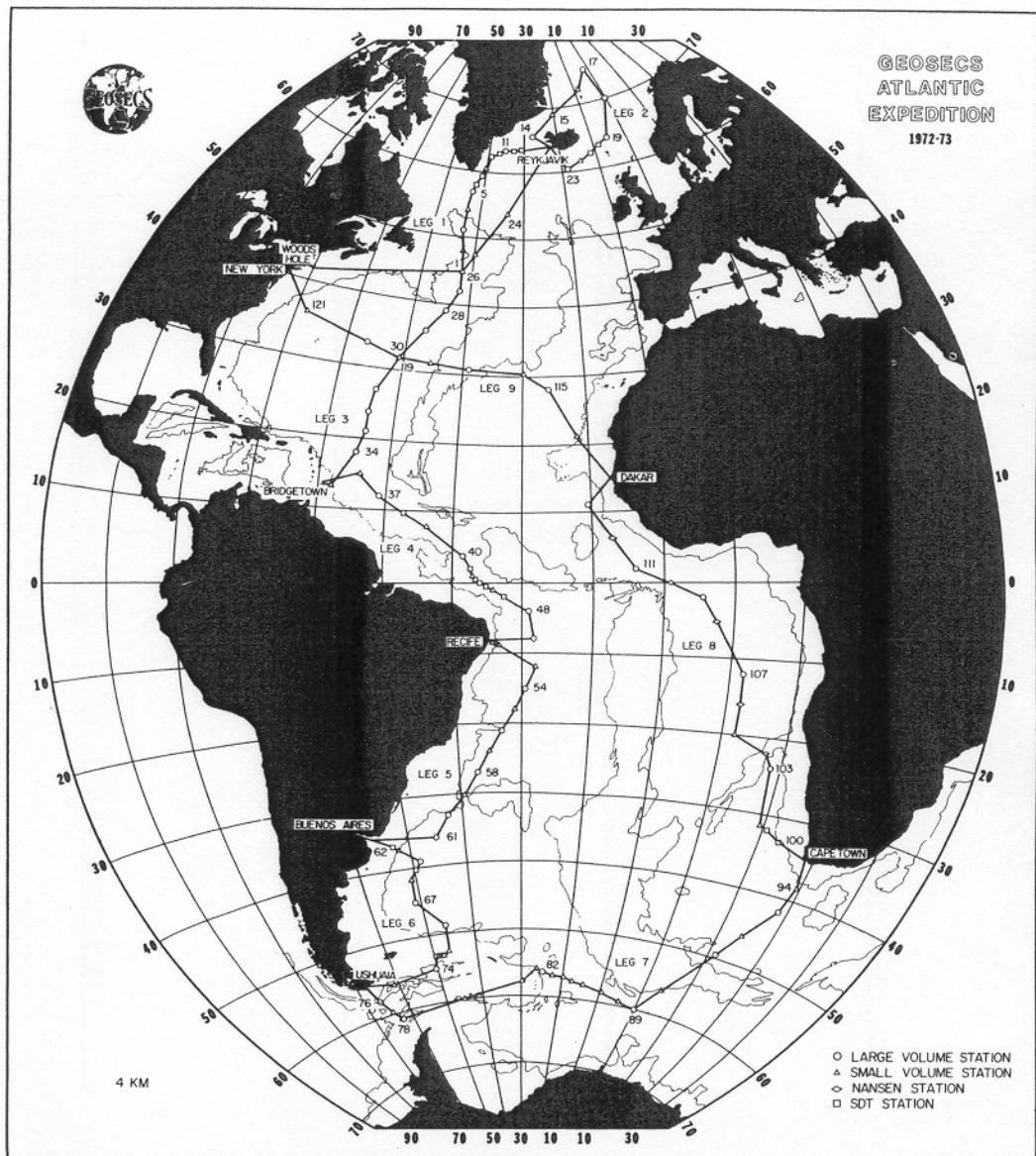


Fig. 1. The locations of the GEOSECS Atlantic stations.

thorium. The mixed precipitate was allowed to settle, separated from the supernatant solution, and returned to the laboratory for analysis.

The following procedure was used to separate, purify, and measure the  $^{228}\text{Th}$ . The iron hydroxide, with its coprecipitated thorium, was dissolved in HCl and separated from the insoluble barium sulfate residue, which contained the radium, by centrifugation. Iron was removed from the thorium fraction by isopropyl ether extraction. The solution was then passed through an anion exchange column to remove uranium. The eluate was evaporated

to a smaller volume ( $\sim 150$  ml), and  $\text{NH}_4\text{OH}$  was added to reprecipitate hydroxides, which were then separated from the solution, dissolved with  $\text{HCl}$ , and passed through a cation exchange column. The thorium fraction, which remained on the column, was eluted with oxalic acid and evaporated to dryness in the presence of  $\text{HNO}_3$  and  $\text{HClO}_4$ . The thorium was then taken up in  $\text{HNO}_3$  and extracted into TTA (thenoyltrifluoroacetone) at a pH of about 2. The TTA was evaporated from a stainless steel disk, creating a thin source of thorium suitable for  $\alpha$  counting.

The following procedure was used to separate, purify, and measure the  $^{228}\text{Ra}$ . The  $\text{BaSO}_4$  fraction of the precipitate was fused with  $\text{Na}_2\text{CO}_3\text{--K}_2\text{CO}_3$ . The carbonate formed was converted to chloride with  $\text{HCl}$ , rinsed, and dissolved in distilled water. The radium solution was freed of all thorium by means of repeated  $\text{Fe}(\text{OH})_3$  precipitations. A  $^{230}\text{Th}$  spike was then added and the solution stored for a known time (about one year), during which  $^{228}\text{Th}$  grew toward equilibrium with its parent  $^{228}\text{Ra}$ . The thorium was then separated by several  $\text{Fe}(\text{OH})_3$  precipitations, processed as described above, and mounted for  $\alpha$  spectrometric measurement.

During the period of  $^{228}\text{Th}$  growth in the radium solution, the  $^{226}\text{Ra}$  content of the solution was determined (as a natural yield tracer for  $^{228}\text{Ra}$ ) by sweeping radon gas accumulated for a known period of time out of the solution with helium carrier. The radon was frozen out in traps cooled by liquid air and was quantitatively transferred to an  $\alpha$  scintillation counter.

The  $^{228}\text{Th}$  content of the sample was calculated from the  $^{228}\text{Th}/^{230}\text{Th}$  ratio measured on the thorium fraction and a knowledge of the amount of  $^{230}\text{Th}$  spike added per unit of seawater. Corrections were made for the extent of  $^{228}\text{Th}$  growth during storage in the precipitate and for decay after laboratory separation. The  $^{228}\text{Ra}$  content was obtained by measuring the  $^{228}\text{Ra}/^{226}\text{Ra}$  ratio in the radium fraction and the "measured" concentration of  $^{226}\text{Ra}$  in seawater samples collected at the station. Because most of the GEOSECS  $^{226}\text{Ra}$  measurements are not from our large volume samples, the "measured"  $^{226}\text{Ra}$  we used is obtained from the correlation between  $^{226}\text{Ra}$  and  $\text{H}_2\text{SiO}_4$  concentrations in the surface Atlantic Ocean (MATHIEU, BAINBRIDGE, BROECKER, HOROWITZ, LI and SARMIENTO, 1977). The "measured"  $^{226}\text{Ra}$  introduces a systematic error of about 5% on  $^{226}\text{Ra}$  values. The blank correction for  $^{228}\text{Ra}$  is about  $0.1 \pm 0.02$  dpm  $(100 \text{ kg})^{-1}$  and for  $^{228}\text{Th}$  about  $0.05 \pm 0.01$  dpm  $(100 \text{ kg})^{-1}$ .

## RESULTS AND DISCUSSION

The  $^{228}\text{Ra}$  and  $^{228}\text{Th}$  concentrations and  $^{228}\text{Th}/^{228}\text{Ra}$  activity ratios at various GEOSECS Atlantic stations are summarized in a table, which can be obtained by request.

The north-south cross sections of  $^{228}\text{Ra}$  and  $^{228}\text{Th}$  concentrations and  $^{228}\text{Th}/^{228}\text{Ra}$  activity ratio along the western and eastern Atlantic tracks are shown in Figs 2, 3, and 4. The regions of high  $^{228}\text{Ra}$  concentration correspond to the northern and southern subtropical warm water masses (Fig. 2). The subsurface water at the equator with extremely low  $^{228}\text{Ra}$  concentration represents the upwelling water mass of the Antarctic Intermediate Water as also suggested by the GEOSECS  $^{14}\text{C}$  data (BROECKER, PENG and STUIVER, 1978). At stations south of the Antarctic Convergence (south of station 76),  $^{228}\text{Ra}$  concentration is always below our analytical detection limit [ $< 0.1$  dpm  $(100 \text{ kg})^{-1}$ , crosses in Fig. 2]. Waters north of the Arctic Convergence (north of station 5) are also relatively poor in  $^{228}\text{Ra}$ . The subsurface maxima of  $^{228}\text{Th}$  are directly under the surface  $^{228}\text{Ra}$

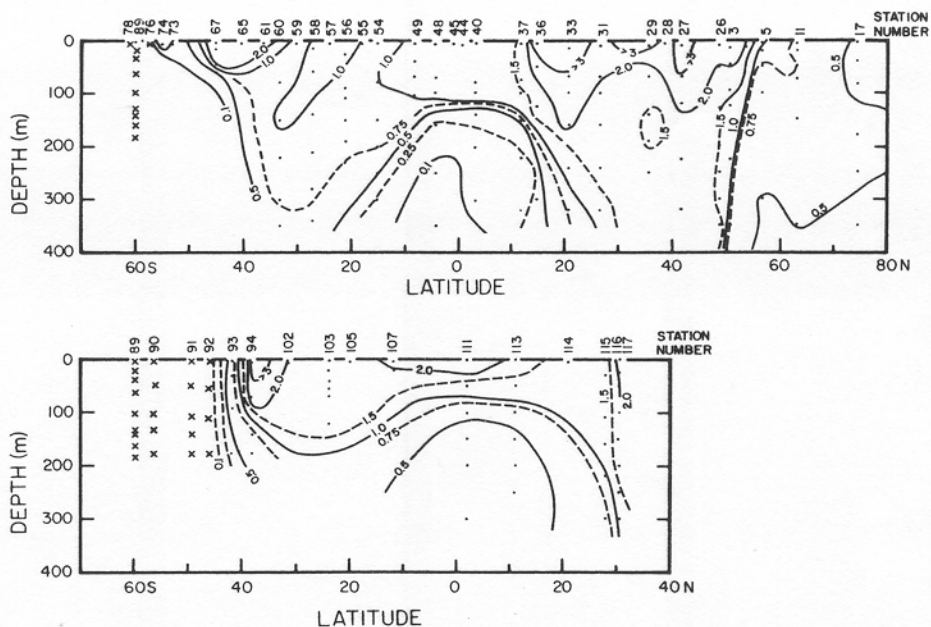


Fig. 2. The N-S sections of  $^{228}\text{Ra}$  concentration data [ $\text{dpm (100 kg)}^{-1}$ ] along the western (top) and the eastern (bottom) Atlantic. The crosses represent  $^{228}\text{Ra}$  concentrations of less than  $0.1 \text{ dpm (100 kg)}^{-1}$ .

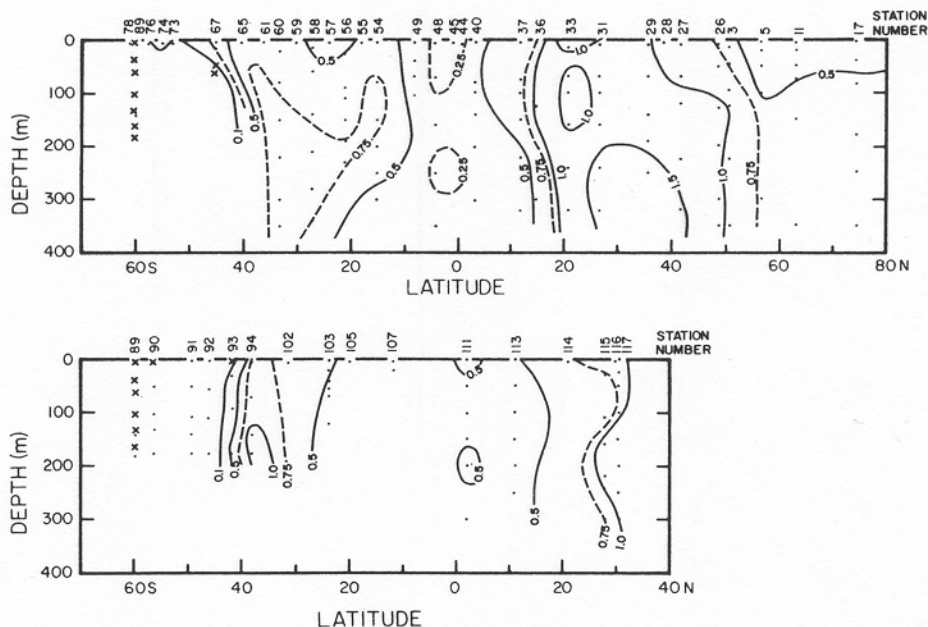


Fig. 3. The N-S sections of  $^{228}\text{Th}$  concentration data [ $\text{dpm (100 kg)}^{-1}$ ] along the western (top) and the eastern (bottom) Atlantic. The crosses represent  $^{228}\text{Th}$  concentrations of less than  $0.02 \text{ dpm (100 kg)}^{-1}$ .

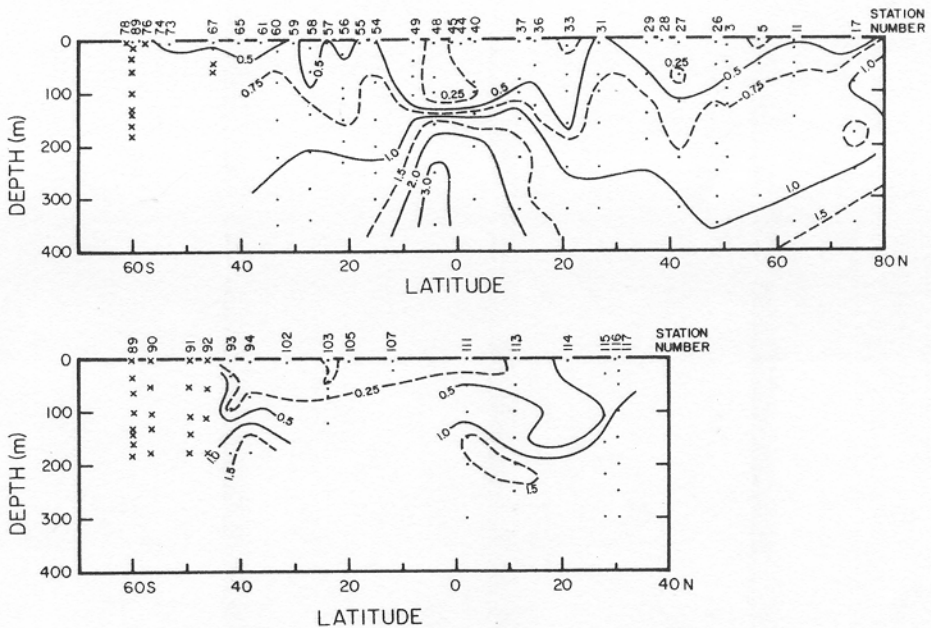


Fig. 4. The N-S sections of the activity ratio of  $^{228}\text{Th}/^{228}\text{Ra}$  along the western (top) and the eastern (bottom) Atlantic. The crosses represent samples with  $^{228}\text{Th}$  and  $^{228}\text{Ra}$  concentrations below detection limits.

maxima at the temperate regions (compare Figs 2 and 3), while  $^{228}\text{Th}/^{228}\text{Ra}$  activity ratios increase from much less than unity at the surface to greater than unity at depths of 200 to 300 m (Fig. 4). Both facts indicate that  $^{228}\text{Th}$  produced continuously by the decay of  $^{228}\text{Ra}$  in the surface layers is removed by settling particles and partially regenerated into the water column at greater depths with little horizontal transport. The extremely high  $^{228}\text{Th}/^{228}\text{Ra}$  activity ratio in the equatorial subsurface water (Fig. 4) corresponds nicely with the oxygen minimum there, suggesting that the regeneration of  $^{228}\text{Th}$  is related to the oxidation of organic matter at depth.

The standing crops or the sums of  $^{228}\text{Ra}$  and  $^{228}\text{Th}$  in the surface water column of 350 m per unit area ( $\sum ^{228}\text{Ra}$  and  $\sum ^{228}\text{Th}$  in  $\text{dpm cm}^{-2}$ ) were obtained by linear interpolation where there are enough data points (Table 1, Fig. 5A). Stations in the north temperate region give the higher  $\sum ^{228}\text{Ra}$  and  $\sum ^{228}\text{Th}$  values.

At a steady state, the deficiency of  $\sum ^{228}\text{Th}$  with respect to  $\sum ^{228}\text{Ra}$  in the upper 350 m should be balanced by a steady vertical particulate flux of  $^{228}\text{Th}$  across the bottom of the surface water column,  $J_{\text{Th}} (= \lambda^{228}\text{Th} [\sum ^{228}\text{Ra} - \sum ^{228}\text{Th}]) \text{ dpm cm}^{-2} \text{ yr}^{-1}$ , where  $\lambda^{228}\text{Th}$  is the decay constant of  $^{228}\text{Th}$ . Stations in the north temperate region usually give high  $J_{\text{Th}}$  values, but exceptions are stations 33, 115, and 117 in the middle of the Sargasso Sea, which give low  $J_{\text{Th}}$  values (Table 1 and Fig. 5B).

Two crosses in Fig. 5B indicate  $^{228}\text{Th}$  fluxes obtained by sediment trap experiments at a depth of about 4000 m at the Atlantic equatorial and Sargasso Sea sites (BREWER, SPENCER, NOZAKI and BACON, 1979). The agreement is remarkable considering the uncertainty involved in both methods. For example, the regeneration of  $^{228}\text{Th}$  below 350 m would

Table 1. The standing crops of  $^{228}\text{Ra}$  and  $^{228}\text{Th}$  down to 350 m ( $\sum^{228}\text{Ra}$  and  $\sum^{228}\text{Th}$ ) and down to  $^{228}\text{Ra}$  minimum ( $\sum^{228}\text{Ra}$ )<sup>\*</sup> and the vertical particulate flux of  $^{228}\text{Th}$  ( $J_{\text{Th}}$ )

Station No.	Latitude	Longitude	$\sum^{228}\text{Ra}$ dpm cm <sup>-2</sup>	$\sum^{228}\text{Th}$ dpm cm <sup>-2</sup>	$J_{\text{Th}}$ 10 <sup>-3</sup> dpm cm <sup>-2</sup> yr <sup>-1</sup>	$\sum^{228}\text{Th}/\sum^{228}\text{Ra}$	$\sum^{228}\text{Ra}$ dpm cm <sup>-2</sup>
17	74°56.0'N	01°07.3'W	0.19	0.19	~0±11	1.0	0.79
19	64 12.0	05 34.2	0.29	0.14	54±4	0.47	0.68
11	63 31.9	35 13.8	0.21	0.19	7±11	0.89	0.73
23	60 24.9	18 37.0	0.41	0.29	44±22	0.71	1.34
5	56 56.7	42 33.5	0.19	0.14	18±8	0.73	0.83
24	53 45.6	33 37.6	0.52	0.26	94±28	0.50	1.40
3	51 01.1	43 07.0	0.48	0.27	76±25	0.56	1.77
26	44 57.6	42 04.6	0.55	0.38	62±29	0.69	1.50
27	42 00.0	42 02.0	0.74	0.43	112±38	0.50	1.35
29	35 58.5	47 00.5	0.67	0.48	69±36	0.72	1.78
120	33 16.0	56 33.0	0.78	0.47	112±40	0.60	1.55
117	30 40.5	38 58.0	0.57	0.43	51±30	0.75	1.06
115	28 01.5	26 00.0	0.34	0.30	15±19	0.89	0.56
31	27 00.0	53 32.0	0.60	0.53	25±34	0.89	1.06
33	21 00.0	54 00.0	0.66	0.37	105±33	0.57	0.94
36	15 00.0	53 56.5	0.50	0.30	73±26	0.59	0.63
37	12 01.8	50 59.8	0.25	0.16	33±13	0.64	0.28
113	10 59.4	20 32.4	0.20	0.14	22±10	0.70	0.22
40	03 56.8	38 31.0	0.21	0.10	40±10	0.50	0.21
111	02 00.0	14 01.3	0.18	0.16	7±10	0.88	0.20
48	04 00.0S	29 00.0	0.16	0.09	25±8	0.53	0.19
54	15 02.5	29 32.0	0.26	0.24	7±14	0.92	0.30
56	21 00.5	33 00.0	0.29	0.22	22±15	0.75	0.36
58	27 00.0	37 01.4	0.30	0.23	25±16	0.76	0.39
60	32 58.0	42 30.5	0.32	0.28	15±18	0.88	0.44
67	44 58.0	51 03.5	0.16	—	—	—	—

\* The averaged uncertainties of  $\sum^{228}\text{Ra}$ ,  $\sum^{228}\text{Th}$ ,  $\sum^{228}\text{Th}/\sum^{228}\text{Ra}$ ,  $\sum^{228}\text{Ra}$  are about 13, 10, 16, and 20% respectively.

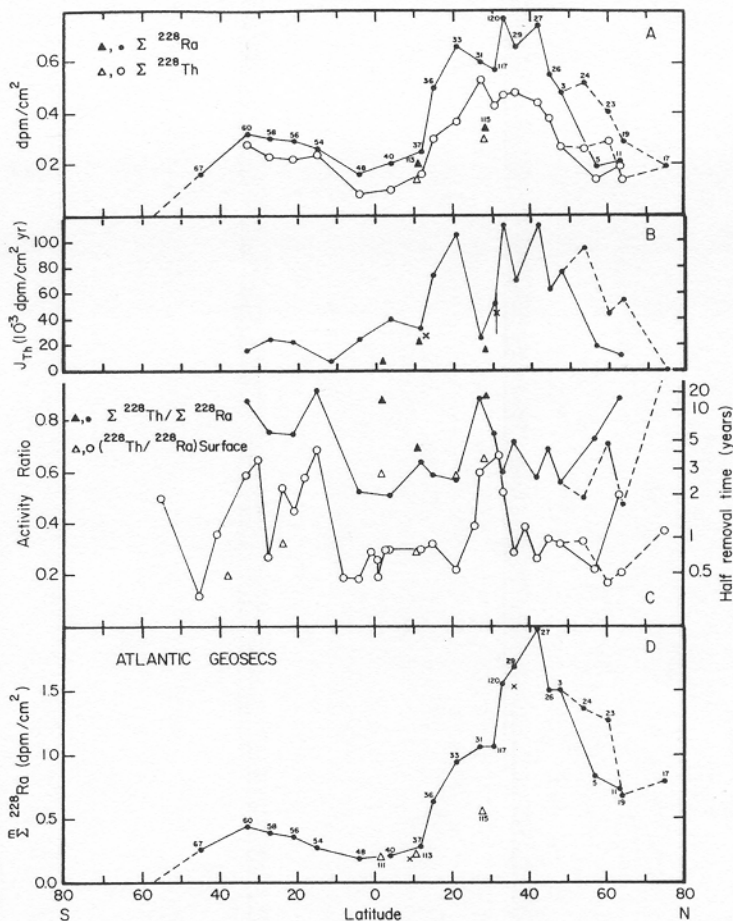


Fig. 5. A. The standing crops of  $^{228}\text{Ra}$  and  $^{228}\text{Th}$  in the upper 350 m. The triangles represent the stations in the eastern Atlantic and the circles in the western Atlantic. The GEOSECS station numbers are indicated. B. The vertical particulate flux of  $^{228}\text{Th}$  across a water depth of 350 m. The two crosses represent values obtained by sediment trap experiments (BREWER *et al.*, 1979). C. The activity ratio of  $\sum^{228}\text{Th}/\sum^{228}\text{Ra}$  (from Fig. 5A) and of  $^{228}\text{Th}/^{228}\text{Ra}$  from the surface waters (<10 m). D. The standing crops of  $^{228}\text{Ra}$  in the water column between the surface and a depth where  $^{228}\text{Ra}$  concentration is nearly zero or a minimum. The two crosses represent the direct measurements by TRIER *et al.* (1972) and MOORE (1972).

make our estimated  $J_{\text{Th}}$  a maximum, while the trapping efficiency of sediment traps is hard to estimate. [According to  $^{230}\text{Th}$  flux obtained by sediment trap, the trapping efficiency may vary around 60 to 80% for  $^{230}\text{Th}$  (SPENCER, BREWER, FLEER, HONJO, KRISHNASWAMI and NAZAKI, 1978 and BREWER *et al.*, 1979).]

The activity ratios of  $\sum^{228}\text{Th}/\sum^{228}\text{Ra}$  in the upper 350 m and of  $^{228}\text{Th}/^{228}\text{Ra}$  in the surface waters (<10 m) are shown in Fig. 5C. The values of  $\sum^{228}\text{Th}/\sum^{228}\text{Ra}$  are always greater than surface  $^{228}\text{Th}/^{228}\text{Ra}$  ratios because of the regeneration of  $^{228}\text{Th}$  within the upper layer. Both ratios are low in the equatorial (10°S ~ 20°N) and the northern region (35 ~ 65°N) of the western Atlantic. The half-removal times of  $^{228}\text{Th}$  by settling particles,  $t_c$ , ( $=t_{1/2}R/[1-R]$ ), where  $t_{1/2}$  = half-life of  $^{228}\text{Th}$ ,  $R$  = activity ratio of  $\sum^{228}\text{Th}/\sum^{228}\text{Ra}$  or

$^{228}\text{Th}/^{228}\text{Ra}$ ; see BROECKER *et al.*, 1973) from these regions are about 0.5 to 1 yr from the surface waters and about 2 to 4 yr from the upper water columns (Fig. 5C). The  $t_c$  in the middle of the Sargasso Sea and the southern temperate zone of the western Atlantic can be as high as 4 yr from the surface waters and about 20 yr from the upper water columns. Comparing the geographical variation of  $t_c$  and the phytoplankton productivity in the Atlantic Ocean (prepared by FAO, 1972), it is evident that  $t_c$  is directly correlated with plankton productivity. High productivity induces high zooplankton grazing and fecal pellet production rates. It has been shown that the sinking of zooplankton fecal pellets is the most important vertical transport mechanism for many reactive radionuclides in the upper layers of the ocean (HIGGO, CHERRY, HEYRAUD and FOWLER, 1977; HIGGO, CHERRY, HEYRAUD, FOWLER and BEASLEY, 1978; CHERRY, FOWLER, BEASLEY and HEYRAUD, 1975; BEASLEY, HEYRAUD, HIGGO, CHERRY and FOWLER, 1978; etc.). In the eastern Atlantic, the data points are too few to generalize about the  $t_c$  variation pattern.

The standing crop of  $^{228}\text{Ra}$  in the water column between the surface and a depth where  $^{228}\text{Ra}$  concentration is near zero or minimum,  $\sum^m {}^{228}\text{Ra}$  (Table 1 and Fig. 5D), was estimated by multiplying  $\sum {}^{228}\text{Ra}$  in the upper 350 m by a factor of  $(\sum {}^3\text{H})_{<350\text{m}}/(\sum {}^3\text{H})_{>350\text{m}}$  at each station, where  $(\sum {}^3\text{H})_{<350\text{m}}$  and  $(\sum {}^3\text{H})_{>350\text{m}}$  are the standing crops of fallout tritium in the water column above and below 350 m, respectively.  $(\sum {}^3\text{H})_{<350\text{m}}/(\sum {}^3\text{H})_{>350\text{m}}$  values at each station were estimated from GEOSECS Atlantic tritium data (ÖSTLUND, DOREY and BRESCHER, 1976). As shown by TRIER, BROECKER and FEELY (1972) and MOORE, FEELY and LI (1980),  $^{228}\text{Ra}$  and  ${}^3\text{H}$  concentrations are linearly correlated in the main thermocline because both radionuclides have been introduced to the upper layers ( $^{228}\text{Ra}$  continuously from the continental shelf sediments and  ${}^3\text{H}$  from the atmosphere for the last 20 yr or so) and dispersed into the water column by the same physical transport processes. In fact, the direct measurements of  $^{228}\text{Ra}$  down to the  $^{228}\text{Ra}$  minimum (crosses in Fig. 5D) at the second GEOSECS intercalibration station ( $36^\circ\text{N}$ ,  $68^\circ\text{W}$ ) in the North Atlantic (TRIER *et al.*, 1972) and in the equatorial Atlantic (MOORE, 1972) agree well with our estimates at the same latitudes.

The total  $^{228}\text{Ra}$  inventory in the Atlantic obtained from Fig. 5D (assuming  $^{228}\text{Ra}$  standing crop is constant along the same latitude if there is only one measurement) is about  $(50 \pm 10) \times 10^{16}$  dpm. The total  $^{228}\text{Ra}$  inventory in the North Atlantic Ocean is about  $(4.5 \pm 0.5)$  times that in the South Atlantic Ocean (Fig. 5D). The area of continental shelf (0 to 200 m, including marginal seas) of the North Atlantic is about four times that of the South Atlantic (FAIRBRIDGE, 1968), also suggesting that the  $^{228}\text{Ra}$  in the surface layers comes from continental shelf sediments (MOORE, 1969). The decay rate of the total  $^{228}\text{Ra}$  in the upper Atlantic ( $= \ln 2/5.75 \times 50 \times 10^{16} = 0.6 \pm 0.1 \times 10^{17}$  dpm yr $^{-1}$ ) divided by the total continental shelf area of the Atlantic Ocean ( $\sim 10^{17}$  cm $^2$ , excluding the Arctic Ocean) gives an average  $^{228}\text{Ra}$  flux of about  $0.6 \pm 0.1$  dpm cm $^{-2}$  yr $^{-1}$  from continental shelf sediments, comparable to  $0.4 \pm 0.1$  dpm cm $^{-2}$  yr $^{-1}$  obtained from the Middle Atlantic Bight by a mass balance calculation (LI, FEELY and SANTSCHI, 1979).

As mentioned before, the vertical profiles of  $^{228}\text{Ra}$  and  $^{14}\text{C}$  (BROECKER *et al.*, 1978) strongly suggest an upward advection of the Antarctic Intermediate Water in the equatorial Atlantic. Non-linear least square fitting of potential temperature profiles from below the surface mixed layer to 500 m (where the salinity vs temperature plot is linear) for stations 37, 40 (western equatorial), and 113 (eastern equatorial) according to MUNK's (1966) steady state vertical advection-diffusion model gives  $K/W = 69 \pm 8$  m and 84 m for the

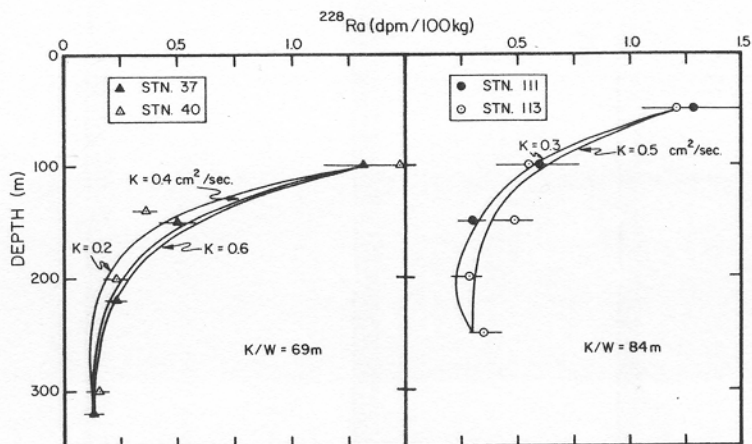


Fig. 6. The fitting of  $^{228}\text{Ra}$  profiles from the eastern (right) and western (left) equatorial Atlantic to MUNK's (1966) vertical advection-diffusion model.

western and eastern equatorial stations, respectively;  $K$  is the vertical eddy diffusion coefficient and  $W$  the vertical advection velocity (positive for upwelling). Adopting these  $K/W$  values,  $^{228}\text{Ra}$  profiles from the same stations can be fitted to MUNK's (1966) model with  $K = 0.4 \pm 0.2 \text{ cm}^2 \text{ s}^{-1}$  (Fig. 6), i.e.,  $W = 18 \pm 9 \text{ m yr}^{-1}$  for the western and  $W = 15 \pm 8 \text{ m yr}^{-1}$  for the eastern equatorial stations. These  $K$  and  $W$  values are consistent with those obtained from the non-steady state vertical advection-diffusion modeling of bomb  $^{14}\text{C}$  (BROECKER *et al.*, 1978).

The  $^{228}\text{Ra}$  concentrations below the surface mixed layer generally decrease exponentially with depth in the Atlantic temperate zones (Fig. 7). At the same water depths, north

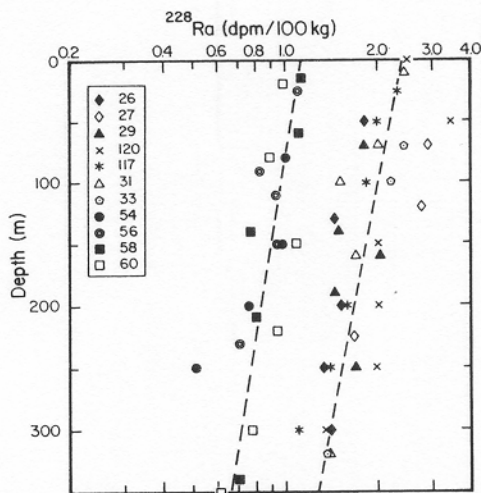


Fig. 7. Depth profiles of  $^{228}\text{Ra}$  from the northern and southern temperate zones.

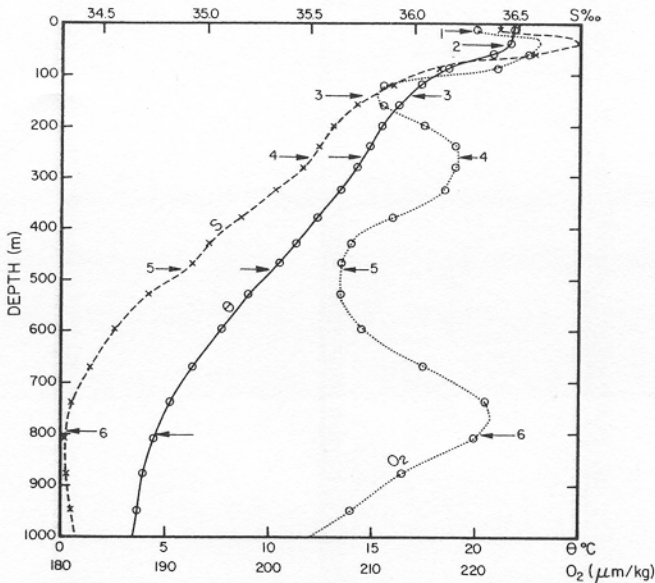


Fig. 8. Depth profiles of potential temperature ( $\theta$ ), salinity ( $S$ ), and  $O_2$  at GEOSECS station 60. The numbers represent inflection points or extrema of  $\theta$ ,  $S$ , and  $O_2$  profiles.

temperate zone waters always have higher  $^{228}\text{Ra}$  concentration than the south temperate zone waters. If one assumes that  $^{228}\text{Ra}$  diffuses downward without advection (KAUFMAN *et al.*, 1973; TRIER *et al.*, 1972; KNAUSS, KU and MOORE, 1978), an apparent vertical eddy diffusion of about  $14 \pm 2 \text{ cm}^2 \text{ s}^{-1}$  is obtained for the temperate zone. However, the simple vertical advection-diffusion model is hardly applicable in the temperate zones. For example, the depth profiles of salinity ( $S^\text{‰}$ ), potential temperature ( $\theta$ ), and oxygen ( $O_2$ ) at station 60 in the southern temperate zone (Fig. 8) show a total of at least six inflection points and extrema between the surface mixed layer and the Antarctic Intermediate Water ( $S$  minimum). Each inflection point or extrema of  $\theta$ ,  $S$  and  $O_2$  occurs roughly at the same water depth (one exception is the third  $O_2$  minimum, which has no corresponding  $\theta$  or  $S$  inflection point or extrema), suggesting that there are at least five water masses interweaving by lateral advection. This also explains the scatter of data points in Fig. 7.

#### SUMMARY

The  $^{228}\text{Ra}$  in the upper water column of the Atlantic Ocean is mainly supplied from continental shelf sediments with an average  $^{228}\text{Ra}$  flux of  $0.6 \text{ dpm cm}^{-2}$  of the continental shelf each year.  $^{228}\text{Ra}$  inputs are mostly accumulated in the northern subtropical warm water mass because about 80% of the continental shelf sediments are in the North Atlantic. Fitting of  $^{228}\text{Ra}$  and potential temperature profiles with MUNK's (1966) vertical advection-diffusion model suggests an upwelling rate of about  $17 \pm 10 \text{ m yr}^{-1}$  and a vertical eddy diffusion coefficient of  $0.4 \pm 0.2 \text{ cm}^2 \text{ s}^{-1}$  in the upper layers of the Atlantic equatorial region.

$^{228}\text{Th}$  is removed from surface waters by settling particles and is partially returned to solution at depths below 100 m in the equatorial region and 200 to 300 m in other regions.

The particulate  $^{228}\text{Th}$  flux reaching the ocean bottom can be as high as  $0.06$  to  $0.11$   $\text{dpm cm}^{-2} \text{yr}^{-1}$  in the northern temperate region (excluding the Sargasso Sea). In the equatorial ( $10^\circ\text{S}$  to  $20^\circ\text{N}$ ) and northern regions ( $35$  to  $65^\circ\text{N}$ ) the half-removal times of  $^{228}\text{Th}$  by settling particles,  $t_c$ , are about  $0.5$  to  $1$  yr from the surface water and about  $2$  to  $4$  yr from the upper  $350$  m. In the other regions,  $t_c$ , can be as high as  $4$  yr from the surface water and about  $20$  yr from the upper  $350$  m. The particles that carry  $^{228}\text{Th}$  downward are probably mostly zooplankton fecal pellets.

*Acknowledgments*—We wish to thank all those who helped collect the water samples on board the R.V. *Knorr* during the GEOSECS expedition. Many thanks are due to Dr W. W. BROECKER and two anonymous reviewers for their helpful comments and suggestions.

The work was supported by NSF Grant OCE 76-04245.

#### REFERENCES

- BEASLEY T. M., M. HEYRAUD, J. J. W. HIGGO, R. D. CHERRY and S. W. FOWLER (1978)  $^{210}\text{Po}$  and  $^{210}\text{Pb}$  in zooplankton fecal pellets. *Marine Biology*, **44**, 325–328.
- BREWER P. G., D. W. SPENCER, Y. NOZAKI and M. P. BACON (1979) Vertical, large particle fluxes of stable and radioactive elements determined from sediment traps. Workshop of Department of Energy on "Processes determining the inputs, behavior and fate of radionuclides and trace elements in continental shelf environments. March 7–9, 1979.
- BROECKER W. S., A. KAUFMAN and R. M. TRIER (1973) The residence time of thorium in surface sea water and its implications regarding the rate of reactive pollutants. *Earth and Planetary Science Letters*, **20**, 35–44.
- BROECKER W. S., T. H. PENG and M. STUIVER (1978) An estimate of the upwelling rate in the equatorial Atlantic based on the distribution of bomb radiocarbon. *Journal of Geophysical Research*, **20**, 6179–6186.
- CHERRY R. D., W. W. FOWLER, T. M. BEASLEY and M. HEYRAUD (1975) Polonium-210: its vertical oceanic transport by zooplankton metabolic activity. *Marine Chemistry*, **3**, 105–110.
- FAIRBRIDGE R. W. (1968) Continents and oceans—statistics of area, volume and relief. In: *The Encyclopedia of Geomorphology*, R. W. Fairbridge, editor, Reinhold Co., 177–186.
- FAO (1972) Atlas of the living resources of the seas. Prepared by Food and Agriculture Organization of the United Nations, Dept. of Fisheries. FAO Fisheries Circular No. 126.
- HIGGO J. J. W., R. D. CHERRY, M. HEYRAUD and S. W. FOWLER (1977) Rapid removal of plutonium from the oceanic surface layer by zooplankton fecal pellets. *Nature, London*, **266**, 623–624.
- HIGGO J. J. W., R. D. CHERRY, M. HEYRAUD, S. W. FOWLER and T. M. BEASLEY (1978) The vertical oceanic transport of alpha-radioactive nuclides by zooplankton fecal pellets. The Natural Radiation Environment III, Houston, Texas, April 23–28.
- KAUFMAN A., R. M. TRIER and W. S. BROECKER (1973) Distribution of  $^{228}\text{Ra}$  in the world ocean. *Journal of Geophysical Research*, **78**, 8827–8848.
- KNAUSS K. G., T. L. KU and W. S. MOORE (1978) Radium and thorium isotopes in the surface waters of the east Pacific and coastal southern California. *Earth and Planetary Science Letters*, **39**, 235–240.
- LI Y. H., H. W. FEELY and P. H. SANTSCHI (1979)  $^{228}\text{Th}$ – $^{228}\text{Ra}$  radioactive disequilibrium in the New York Bight and its implications for coastal pollution. *Earth and Planetary Science Letters*, **42**, 13–16.
- MATHIEU G., A. E. BAINBRIDGE, W. S. BROECKER, R. M. HOROWITZ, Y. H. LI and J. SARMIENTO (1977) GEOSECS Atlantic and Pacific surface hydrography and radon atlas. GEOSECS Operation Group publication No. 120.
- MOORE W. S. (1969) Oceanic concentrations of  $^{228}\text{Ra}$ . *Earth and Planetary Science Letters*, **6**, 437–446.
- MOORE W. S. (1972) Radium-228: application to thermocline mixing studies. *Earth and Planetary Science Letters*, **16**, 421–422.
- MOORE W. S., H. W. FEELY and Y. H. LI (1980) Radium isotopes in sub-arctic waters. *Earth and Planetary Science Letters* (in press).
- MUNK W. H. (1966) Abyssal recipes. *Deep-Sea Research*, **13**, 707–730.
- ÖSTLUND H. G., H. G. DOREY and R. BRESCHER (1976) GEOSECS Atlantic radiocarbon and tritium results. Data Report 5, Tritium Lab., University of Miami, Florida.
- SPENCER D. W., P. G. BREWER, A. FLEER, S. HONJO, S. KRISHNASWAMI and Y. NAZAKI (1978) Chemical fluxes from a sediment trap experiment in the deep Sargasso Sea. *Journal of Marine Research*, **36**, 493–523.
- TRIER R. M., W. S. BROECKER and H. W. FEELY (1972) Radium-228 profile at the second GEOSECS intercalibration station, 1970, in the North Atlantic. *Earth and Planetary Science Letters*, **16**, 141–145.